Thermal Response to Fire of Insulated Cylindrical Steel Elements

FREDERICK W. MOWRER*
Department of Fire Protection Engineering
University of Maryland, College Park, MD 20742, USA

ABSTRACT: Standard calculation methods are used in current design practice in the United States to determine the fire resistance rating of structural steel elements protected with spray-applied fire resistive materials (SFRMs). These calculation methods are based on simplified analysis of heat transfer through the SFRM material to the steel substrate. This analysis assumes one-dimensional heat transfer in Cartesian coordinates, i.e., a flat plate. Based on this analysis, the ratio of the weight per unit length to the surface area per unit length, expressed in terms of the 'W/D ratio,' is the governing parameter for heating of the steel element. For cylindrical rods, such as those used in steel bar joists, and other small structural shapes, this analysis is inappropriate because the surface area of the insulated element increases with increasing insulation thickness, thus increasing the surface area for heat transfer to the insulated assembly. Simplified and detailed numerical heat transfer analyses have been performed in both Cartesian and cylindrical coordinates that demonstrate the reduced level of fire resistance associated with a given thickness of insulation on a cylindrical rod relative to a wide-flange element with the same W/D ratio.

KEY WORDS: structural fire safety, fire resistance, heat transfer.

INTRODUCTION

A NUMBER OF methods have been developed and used to insulate structural steel members from fire exposure and thereby impart a level of fire resistance to the insulated member. Historically, the most common methods of insulation have included concrete encasement, envelopment in gypsum plaster or gypsum wallboard membranes and spray application of light-weight cementitious or mineral fiber spray-applied fire resistive

*E-mail: fmowrer@umd.edu

1042-3915/07/02 0129–15 $10.00/0 DOI: 10.1177/1042391506069337

materials (SFRMs). This last method has become the most widely used method for the 'fireproofing' of structural steel. Under fire conditions, all these protection methods retard the transfer of heat to steel elements through some combination of heat capacity, dehydration, and low thermal conductivity.

The performance of different insulation materials under fire conditions is normally evaluated by subjecting representative insulated elements or assemblies to standard exposure conditions in large-scale fire resistance tests. In the United States, the standard exposure conditions are represented in terms of the standard gas temperature history specified in the ASTM E119 [1] fire resistance test standard. The level of fire resistance imparted by different types and thicknesses of insulating materials is generally expressed in terms of the time period, e.g., 1 h, 2 h, etc., that the element or assembly withstands the standard exposure conditions without exceeding any of the endpoint failure criteria specified in the fire resistance test standard.

The ASTM E119 standard generally requires structural elements to be loaded in a manner consistent with design loading conditions, but includes alternative tests of the protection of structural steel columns and structural steel solid beams and girders to evaluate the assembly without application of design load. Instead, steel temperatures are measured at a number of specified locations, with the criteria that the average temperature at any one cross-section of the structural steel element cannot exceed 538°C (1000°F) and any individual temperature cannot exceed 649°C (1200°F) during the period of fire exposure for which classification is desired.

As an alternative to large-scale fire testing, analytical methods have been developed to calculate equivalent fire resistance ratings for structural steel elements [2–4]. These analytical methods are semi-empirical in that they apply fire test data along with simplified heat transfer theory to the calculation of fire resistance ratings. These analytical methods are based on one-dimensional heat transfer in wide-flange elements, but they are sometimes applied to small elements, such as cylindrical steel rods in bar joists and trusses, despite cautions [4 (Section C5.2.2)] that such application may not be conservative due to geometric effects.

The purpose of this article is to demonstrate that the semi-empirical analytical methods currently used to calculate equivalent fire resistance ratings for structural steel elements are inappropriate for direct application to small structural elements, such as cylindrical rods in steel bar joist assemblies. The analysis in this article also supports the use of 'adjustment factors' that might be used, with further validation, to allow the continued use of the current calculation methods with appropriate adjustments. To this end, simplified and detailed numerical heat transfer models are developed in both Cartesian and cylindrical coordinates, with results of the calculations for these different geometries compared.

BACKGROUND

ASCE/SFPE Standard 29-99 [4] presents a compilation of standard calculation methods for structural fire protection used in the United States. Chapter 5 of this document addresses standard methods for determining the fire resistance of structural steel construction. These methods are adopted by reference in the two current model building codes in the United States, the International Building Code [5], and NFPA 5000 [6]. For structural steel columns and trusses protected with SFRMs, the fire resistance rating is calculated as:

$$R = \left(C_1 \frac{W}{D} + C_2\right)\delta_i \tag{1}$$

Equation (1) suggests a linear relationship between fire resistance rating and insulation thickness.

The commentary in the ASCE/SFPE 29-99 standard notes that 'especially for smaller shapes, the fire resistance of pipe and tubular columns protected with spray-applied materials will be somewhat less than the fire resistance of a wide-flange column with the same weight-to-heated-perimeter ratio (W/D) and thickness of protection. In general, the difference is due to heat transfer principles related to the geometry of the cross-sections. As a result, different material-dependent constants are required . . .'. However, the ASCE/SFPE 29-99 standard does not provide this same caveat for small structural elements used in steel trusses. Buchanan [7, p. 180] addresses this issue in general by noting that 'the section factor F/V (editorial note: F/V is analogous to the W/D ratio) should strictly be calculated using the fire exposed perimeter rather than the inside face of the insulation material, but the inside perimeter is more often used because it is published in tables . . .'. Thus, the issue of geometric effects on heat transfer to insulated steel elements has been recognized, but its impact has not adequately been addressed.

ANALYSIS

Two analytical methods to evaluate heat transfer through fireproofing materials are described in both Cartesian and cylindrical coordinates. The first method is a simplified analysis based on the assumption of

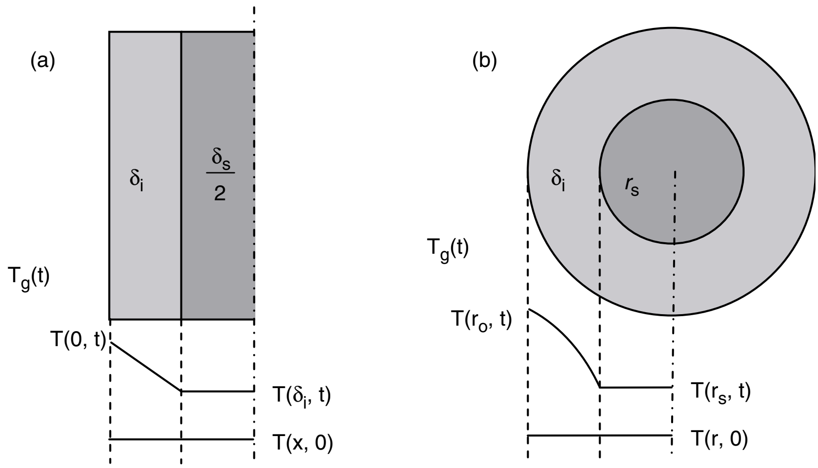

Figure 1. *(a) Schematic illustration of parameters for Cartesian coordinates and (b) schematic illustration of parameters for cylindrical coordinates.*

quasi-steady heat transfer through the insulation material, while the second method is a more detailed numerical finite-difference analysis of transient heat transfer through the insulation. For both coordinate systems, one-dimensional heat transfer is assumed. In the case of Cartesian coordinates, heat is transferred normal to the surface into the insulation and the steel substrate as illustrated in Figure 1(a). In the case of cylindrical coordinates, heat is transferred radially from the outside surface through the insulation and into the steel core, as illustrated in Figure 1(b).

In the Cartesian case, the area through which heat is transferred remains constant through the thickness of the insulation material. In the cylindrical case, the area becomes more concentrated as heat flows from the outer surface of the insulation to the steel core. Since the heated perimeter used in Equation (1) is based on the inside surface area of the insulation, one consequence of this is that the area through which heat is transferred at the exposed surface of the insulation is larger than the heated perimeter of the rod in the cylindrical case. On one hand, the consequence of this would be an underestimation of the rate of heat transfer to the steel core and an overprediction of the fire resistance time. On the other hand, there is more material to absorb heat with increasing radius and this additional heat capacity may tend to offset the increased heat transfer area associated with cylindrical coordinates. Analysis is needed to evaluate which effect is more important.

Simplified Quasi-Steady Analysis

This simplified analysis ignores the heat capacity of the insulation material, thus treating the heat transfer through the insulation material as quasi-steady, and treats the steel element as a lumped capacity with a uniform temperature of T_s. This approach has been used before [2,7,8]. Due to the relatively low density and thermal conductivity of typical SFRMs, a further simplification is to assume that the exposed surface of the insulation material is at the same temperature as the fire gases, T_g, exposing the assembly. With these assumptions, the quasi-steady energy balance on the structural steel element per unit length can be written as

$$\frac{\dot{Q}_k}{L} = \frac{\dot{Q}_s}{L} \tag{2}$$

where $\dot{Q}_k/L$ is the quasi-steady rate of heat conduction through the insulation material to the steel element per unit length of the element, and $\dot{Q}_s/L$ is the rate of heat absorption by the steel element per unit length. The rate of heat absorption by the steel element is expressed in terms of the sensible heating of the element as

$$\frac{\dot{Q}_s}{L} = \rho_s c_{ps} \frac{V_s}{L} \frac{dT_s}{dt} \tag{3}$$

where V_s/L is the volume of the steel element per unit length, which is simply the cross-sectional area of the element, A_{xs} (m^2).

In Cartesian coordinates, the quasi-steady one-dimensional rate of heat transfer through the insulation material per unit length is expressed as

$$\frac{\dot{Q}_k}{L} = -k_i \frac{A_p}{L} \frac{\Delta T}{\Delta x} = \frac{k_i D}{\delta_i} \left(T_g - T_s\right) \tag{4}$$

where A_p/L is the surface area per unit length of the steel element, which is defined as the heated perimeter of the steel element, $D \equiv A_p/L$ (m), and $\Delta T/\Delta x$ is the temperature gradient through the insulation material, which is evaluated under quasi-steady conditions as $(T_g - T_s)/\delta_i$ (°C/m).

In cylindrical coordinates, the quasi-steady one-dimensional rate of heat transfer through the insulation material per unit length is expressed as

$$\frac{\dot{Q}_k}{L} = -k_i \frac{A}{L} \frac{dT}{dr} = \frac{2\pi k_i}{\ln(r_o/r_s)} \left(T_g - T_s\right) \tag{5}$$

where r_s is the radius of the cylindrical steel element (m) and r_o is the outside radius of the insulated assembly (m), such that $r_o = r_s + \delta_i$.

For the Cartesian coordinate case, Equations (3) and (4) are equated and rearranged to solve for the rate of temperature rise:

$$\left(\frac{dT_s}{dt}\right)_{Cart} = \frac{k_i(T_g - T_s)}{\delta_i(\rho_s c_{ps}\delta_s/2)} \tag{6}$$

For cylindrical coordinates, the rate of temperature rise is determined by equating and rearranging Equations (3) and (5):

$$\left(\frac{dT_s}{dt}\right)_{cyl} = \frac{2k_i(T_g - T_s)}{\rho_s c_{ps} r_s^2 \ln(r_o/r_s)} \tag{7}$$

The W/D ratio represents the weight of an element per unit length, $W \equiv \rho_s V_s/L$, divided by the heated perimeter of the element per unit length, which is defined earlier. For a flat plate being heated on both faces (but not the ends), the W/D ratio becomes $(W/D)_{Cart} = \rho_s\delta_s/2$; for a cylindrical rod, the W/D ratio can be expressed as $(W/D)_{cyl} = \rho_s r_s/2$.

Substituting these definitions for the W/D ratios, characteristic time constants for the Cartesian and cylindrical cases can be defined based on Equations (6) and (7) as

$$\tau_{Cart} = \frac{\rho_s c_{ps}\delta_s\delta_i}{2k_i} = \frac{c_{ps}\delta_i}{k_i}\left(\frac{W}{D}\right)_{Cart} \tag{8}$$

$$\tau_{cyl} = \frac{\rho_s c_{ps} r_s^2 \ln(r_o/r_s)}{2k_i} = \frac{c_{ps} r_s \ln(r_o/r_s)}{k_i}\left(\frac{W}{D}\right)_{cyl} = \frac{c_{ps} r_s \ln(1 + \delta_i/r_s)}{k_i}\left(\frac{W}{D}\right)_{cyl} \tag{9}$$

With these definitions for the characteristic time constants, the differential Equations (6) and (7) expressing the rate of rise of the steel temperature become:

$$\frac{dT_s}{dt} = \frac{T_g - T_s}{\tau} \tag{10}$$

For most realistic boundary conditions, Equation (10) will require numerical solution, but closed-form analytical solutions exist for some idealized boundary conditions. For the case of a constant gas temperature, the analytical solution for Equation (10) is

$$\frac{\Delta T_s}{\Delta T_g} = 1 - \exp\left(\frac{t}{\tau}\right) \tag{11}$$

For a gas temperature that varies linearly with time, $\Delta T_g = bt$, the analytical solution for Equation 10 can be expressed as

$$\frac{\Delta T_s}{\Delta T_c} = \exp\left(-\frac{t}{\tau}\right) + \left(\frac{t}{\tau} - 1\right) \tag{12}$$

where $\Delta T_c = b\tau$. For a given W/D ratio, the relationship between the cylindrical and Cartesian time constants, and consequently, the heating rates, can be expressed as

$$\frac{\tau_{cyl}}{\tau_{Cart}} = \frac{\ln(1 + \delta_i/r_s)}{\delta_i/r_s} \tag{13}$$

The relationship expressed by Equation (13) is illustrated in Figure 2.

Figure 2 shows that the time constant for a cylindrical rod will be smaller than the time constant for a flat plate with the same W/D ratio, with the difference increasing with increasing insulation thickness or decreasing rod diameter. Physically, this means that the cylindrical rod will heat up faster than a flat plate with the same W/D ratio and consequently will have a lower fire resistance based on the achievement of a critical steel temperature. This is illustrated in terms of the following example.

Consider a cylindrical steel rod with a diameter of 28 mm protected with 19 mm of a mineral fiber SFRM. Assume the steel rod has a density of $\rho_s = 7850\,kg/m^3$ and a constant specific heat of $c_{ps} = 0.6\,kJ/kg\,K$, while the

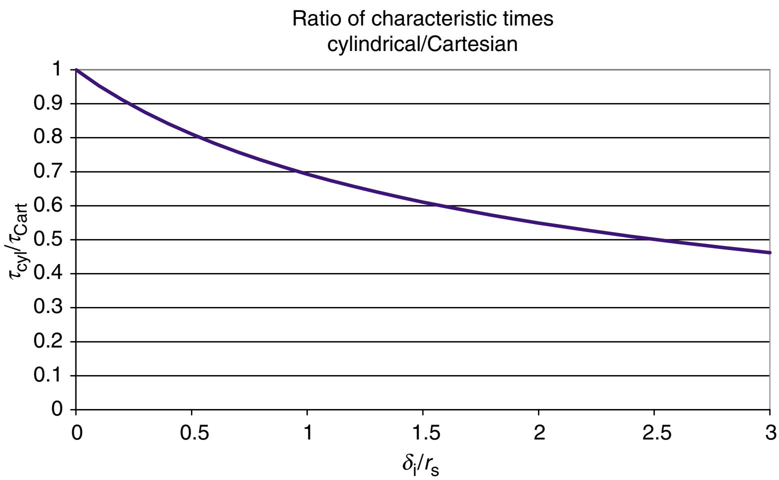

Figure 2. *Ratio of cylindrical to Cartesian characteristic times as a function of the ratio of insulation thickness to cylinder radius. (The color version of this figure is available online.)*

insulation material has a thermal conductivity of $k_i = 0.12 \times 10^{-3}$ kW/m K. Based on these assumed properties, which are taken from Buchanan [7], the W/D ratio and the time constant for the insulated steel rod are calculated to be $(W/D)_{\mathrm{cyl}} = 54.95\,\mathrm{kg/m^2}$ and $\tau_{\mathrm{cyl}} = 3298\,\mathrm{s}$. A flat plate with the same W/D ratio would have a time constant of $\tau_{\mathrm{Cart}} = 5220\,\mathrm{s}$.

Next, the time it would take for these elements to reach a critical temperature of 538°C (i.e., $\Delta T_{\mathrm{s,cr}} = 538 - 20 = 518$°C) if they were suddenly immersed in fire environments with constant gas temperatures ranging from 620 to 1020°C (i.e., $\Delta T_{\mathrm{g}} = 600$ to 1000°C) is considered. Equation (11) is inverted to calculate these critical times as

$$t_{\mathrm{cr}} = -\tau \cdot \ln\left(1 - \frac{\Delta T_{\mathrm{s,cr}}}{\Delta T_{\mathrm{g}}}\right) \tag{14}$$

The results of this example case are shown in Table 1. As evident from Equation (14), the time to reach the critical steel temperature for this example varies linearly with the time constant. From Equation (13), for this example the relationship between the two time constants is $\tau_{\mathrm{cyl}} = 0.63\tau_{\mathrm{Cart}}$. This relationship is borne out by the results shown in Table 1.

Now consider what would happen if the insulation thickness is doubled to 38 mm with all other properties remaining the same. The W/D ratio would remain the same and the new characteristic times would be calculated as $\tau_{\mathrm{Cart}} = 10{,}440\,\mathrm{s}$ and $\tau_{\mathrm{cyl}} = 5047\,\mathrm{s}$ in accordance with Equations (8) and (9). Note that the time constant for the cylindrical case is only a factor of 1.53 times the previous value due to the logarithmic relationship in Equation (9), while the time constant for the Cartesian case is twice the previous value due to the linear relationship between insulation thickness and time constant expressed in Equation (8). This demonstrates the diminishing returns associated with increased insulation thickness for cylindrical elements resulting from the increasing heat transfer surface area with increasing insulation thickness.

Table 1. Calculated times to critical steel temperature for simplified example case.

Gas temperature rise, ΔT_{g} (°C)	Time to $\Delta T_{\mathrm{s,cr}} = 518$°C – cylindrical (min)	Time to $\Delta T_{\mathrm{s,cr}} = 518$°C – Cartesian (min)
600	109	173
700	74	117
800	57	91
900	47	75
1000	40	63

Detailed Transient Analysis

The simplified quasi-steady analysis presented earlier does not take into account the heat capacity effects of the insulation material or the variable material properties of the insulation material and the steel. To evaluate these effects, a more detailed analysis of the transient heat transfer through an SFRM material was conducted. This more detailed transient analysis involved the development of one-dimensional numerical heat transfer calculations in both Cartesian and cylindrical coordinates and the implementation of these calculations in spreadsheet templates.

Space does not permit a full description here of the numerical implementation of the detailed transient heat transfer calculations. By using a typical explicit finite-difference scheme to represent the governing one-dimensional conduction equations for Cartesian and cylindrical coordinates for the case of variable thermal properties, the following results are obtained:

$$\rho_i c_\mathrm{i} \frac{\partial T}{\partial t} = \frac{\partial}{\partial x}\left(k_\mathrm{i} \frac{\partial T}{\partial x}\right) \tag{15}$$

$$\rho_\mathrm{i} c_\mathrm{i} \frac{\partial T}{\partial t} = \frac{1}{r}\frac{\partial}{\partial r}\left(k_\mathrm{i} r \frac{\partial T}{\partial r}\right) \tag{16}$$

These equations require an initial condition and two boundary conditions to solve. The initial condition is that the temperatures throughout the insulation and the steel are at ambient temperature, $T_\mathrm{o} = 20°\mathrm{C}$ at time $t = 0$. The boundary condition at the exposed surface of the insulation is a radiative–convective boundary condition, which can be expressed as

$$k_\mathrm{i} \frac{\partial T}{\partial \eta} = h_\mathrm{c}\left(T_\mathrm{g} - T\right) + \varepsilon\sigma\left(T_\mathrm{g}^4 - T^4\right) \tag{17}$$

where T is the temperature of the exposed surface of the insulation. From a practical standpoint, the boundary condition $T = T_\mathrm{g}$ at the insulation surface, which is the boundary condition specified for the simplified quasi-steady analysis, would also be appropriate here due to the relatively low thermal conductivity of typical spray-applied insulation materials, but the more exact boundary condition expressed by Equation (17) was used for the numerical calculations. This serves as a check on the validity of the temperature boundary condition used in the simplified analysis. The other boundary condition is that the heat transferred to the steel element is absorbed and acts to sensibly heat the steel element uniformly; in cylindrical coordinates, this boundary condition is expressed as

$$\rho_s c_{ps} \frac{\partial T_s}{\partial t} = \frac{2k_i}{r_s} \frac{\partial T}{\partial r}\bigg|_{r=r_s} \tag{18}$$

For comparison purposes, the same insulation thickness and material properties, the same structural element sizes, and the same constant gas temperatures that were used for the simplified example calculations are used to perform detailed numerical example calculations. For the detailed transient calculations, the density and specific heat of the insulation material are also needed. For these calculations, the density of the insulation material was specified as $\rho_i = 240\,\mathrm{kg/m^3}$ and the specific heat of the insulation material was specified with a constant value of $c_i = 1.2\,\mathrm{kJ/kg\,K}$. Buchanan [7] suggests these values are representative for a mineral fiber SFRM. Specific thermal properties associated with a particular SFRM should be used if available, but such properties are not generally available. The calculated times for the insulated steel elements to reach the critical steel temperature of 538°C are shown in Table 2 for the detailed transient analysis of the cylindrical and Cartesian cases with these specified constant material properties. The ratios between the foregoing times to reach the critical temperature of 538°C are also shown in Table 2.

Note that the times to reach the critical steel temperature based on the detailed transient analysis are greater than the comparable times for the simplified quasi-steady analysis listed in Table 1. In general, the times based on the transient analysis are about 12–15% longer than the comparable times based on the quasi-steady analysis. This is to be expected because the simplified quasi-steady analysis neglects the thermal penetration time associated with the detailed transient analysis and consequently overestimates the rate of heat transfer to the steel element during the early

Table 2. Calculated times to critical steel temperature for detailed transient example case.

Gas temperature rise, ΔT_g (°C)	Time to $\Delta T_{s,cr} = 518$°CC – cylindrical (min)	Time to $\Delta T_{s,cr} = 518$°C – Cartesian (min)	Ratio of times to critical temperature
600	122	193	0.63
700	83	130	0.64
800	64	101	0.63
900	53	83	0.64
1000	46	71	0.65

stage of heating. In general, the thermal penetration time will depend on the thickness and the thermal diffusivity of the insulation material as

$$t_p \sim \left(\frac{\delta_i^2}{\alpha_i}\right) \tag{19}$$

where $\alpha_i \equiv k_i/(\rho_i c_{pi})$ is the thermal diffusivity of the insulation material, which evaluates to $4.2 \times 10^{-7}\,m^2/s$ for the insulation properties used for the example calculations.

The ratios of the times to reach the critical steel temperature based on the detailed transient analysis are shown for the Cartesian and cylindrical coordinates in Table 2, for each gas temperature case. These values are all consistent with the expected value for this ratio of 0.63 based on Equation (13). This suggests that Equation (13) might be used to adjust the fire resistance ratings of cylindrical rods that have been established based on the W/D concept as represented by Equation (1). Before this is done, however, further analysis should be conducted for a range of boundary conditions, rod diameters and insulation thicknesses to evaluate how generally applicable these results are. Such calculations should also be compared with experimental results.

Transient temperature histories were also calculated for the cylindrical and Cartesian cases in response to the ISO 834 standard time–temperature curve. The results of these calculations are shown in Figure 3(a) and (b), with the vertical arrows in each figure denoting the respective times to reach an assumed critical steel temperature of 538°C.

Additional calculations were performed using variable temperature-dependent material properties for the insulation material and the steel. For these calculations, the following temperature-dependent material properties, based on Milke [8] and Jeanes [9], were used:

$$k_i = 0.04 + 2 \times 10^{-4} T\ (^\circ C)$$

$$c_i = 0.879 + 0.00066T\ (^\circ C)$$

$$c_{ps} = 0.420 + 0.00051T\ (^\circ C)$$

The results of the detailed transient calculations using temperature-dependent material properties are summarized in Figure 4, which shows the calculated times to reach critical steel temperatures of 538°C as well as 593°C for a steel element with a W/D ratio of $54.95\,kg/m^2$. The ASTM E119 standard specifies 593°C as the average steel temperature for acceptance of loaded floor and roof specimens employing structural steel. Results of the

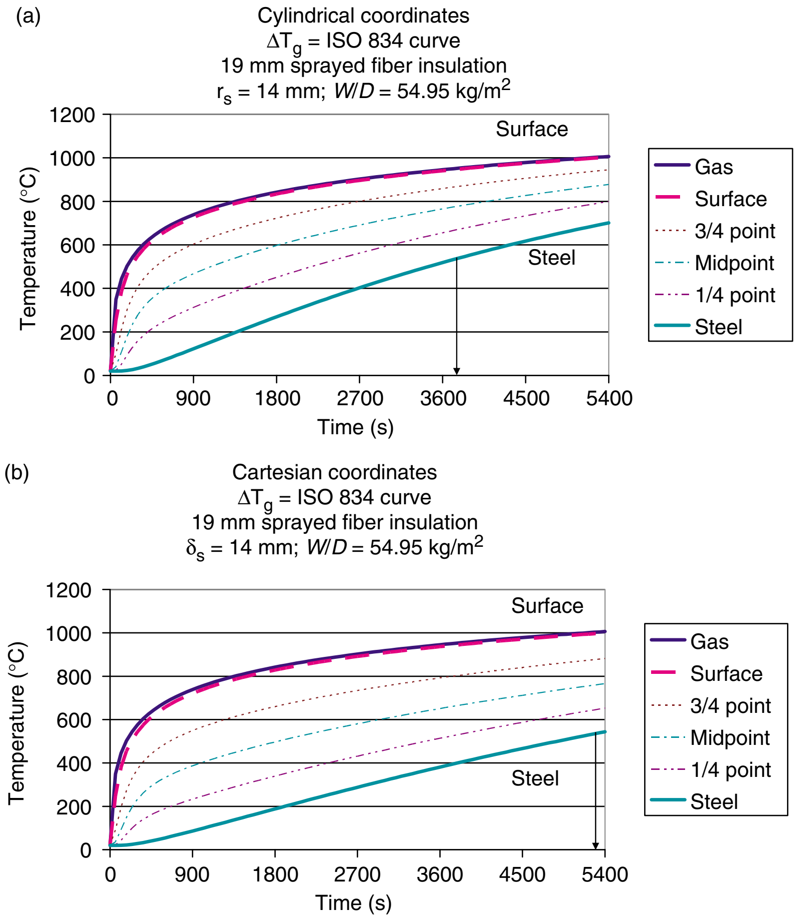

Figure 3. *(a) Example of detailed transient analysis calculations for cylindrical case in response to ISO 834 gas temperature and (b) example of detailed transient analysis calculations for Cartesian case in response to ISO 834 gas temperature. (The color version of this figure is available online.)*

calculations for Cartesian and cylindrical coordinates are shown as a function of the insulation thickness. The ratios between these times to reach critical temperatures are also shown in Figure 4, along with the results of Equation (13). These ratios demonstrate not only the diminishing returns associated with increasing insulation thickness for cylindrical elements noted above, but also that these effects are not as pronounced as indicated by Equation (13). This is due to the added heat capacity effects associated with increasing insulation thicknesses that are not considered in Equation (13). A consequence of this is that Equation (13) should

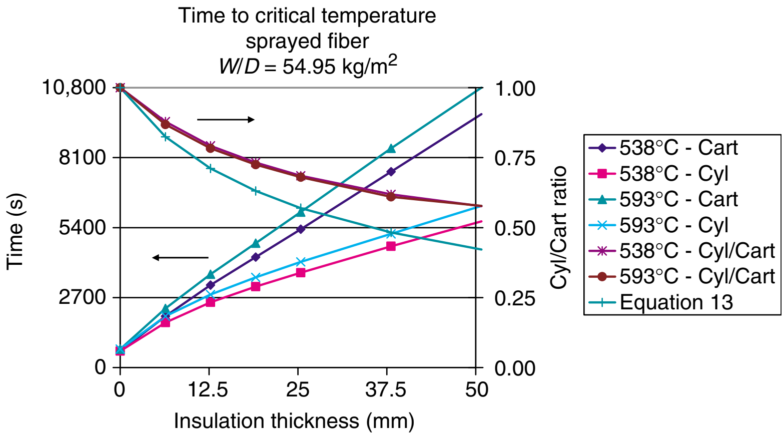

Figure 4. *Times to reach critical steel temperatures of 538 and 593°C based on detailed transient calculations with temperature-dependent material properties and ratios between these times for cylindrical and Cartesian elements. (The color version of this figure is available online.)*

provide a conservative estimate of the effects of geometry on the fire resistance of insulated structural steel elements.

SUMMARY AND CONCLUSIONS

The current design basis used in the United States for the fire resistance of structural steel elements based on W/D ratios has been reviewed. This design basis is incorporated in the ASCE/SFPE 29-99 standard [4], which is adopted by reference in the two current model building codes [5,6] in the United States. These methods are based on the work of Lie and Stanzak [2], who compared a number of simplified calculation methods with a more detailed numerical analysis to develop the 'W/D concept' more than 30 years ago. This work as well as subsequent development work on the W/D concept [3] was based largely on wide-flange structural steel elements with relatively large rectilinear shapes. The W/D concept is sometimes applied to elements with cylindrical shapes, such as steel rods in bar joists, and other small shapes despite longstanding recognition that such applications might not be conservative due to the geometric effects addressed in this work.

Simplified and detailed numerical heat transfer models were developed to evaluate the geometric effects associated with heat transfer through insulation materials to a steel structural element in both Cartesian and cylindrical coordinates. Calculations performed with these models demonstrate that the temperature of the steel element increases more rapidly for small cylindrical elements than for wide-flange elements with the same W/D

ratio due to geometric effects. It appears that this difference can be evaluated conservatively in terms of Equation (13), but further work is needed to determine how generally this relationship applicable is for other insulation thicknesses, material properties, rod diameters (or other small structural shapes), and boundary conditions.

NOMENCLATURE

A = area (m^2)
c_p = specific heat (kJ/kg K)
C_1 = SFRM material constant
C_2 = SFRM material constant
D = heated perimeter length (m)
h_c = heat transfer coefficient (kW/m^2 K)
k = thermal conductivity (kW/m K)
L = length (m)
$\dot{Q}$ = rate of energy transfer (kW)
r = radius or radial position (m)
R = fire resistance rating (h)
t = time (s)
T = temperature (°C or K)
V = volume (m^3)
W = weight per unit length (kg/m)
x = dimension into insulation (m)

GREEK

α = thermal diffusivity (m^2/s)
δ = thickness (m)
ε = emissivity
ρ = density (kg/m^3)
σ = Stefan–Boltzmann constant
τ = characteristic time constant (s)

SUBSCRIPTS

Cart = Cartesian
cr = critical
cyl or Cyl = cylindrical
g = gas
i = insulation

k = conducted
o = ambient, outer
p = perimeter
r = radial
s = steel
xs = cross-section

REFERENCES

1. "Standard Test Methods for Fire Tests of Building Construction and Materials," ASTM E119-00a, ASTM International, West Conshohocken, PA, 2000.
2. Lie, T.T. and Stanzak, W.W., "Fire Resistance of Protected Steel Columns," Eng. J. American Institute of Steel Construction, Vol. 10, 1973, pp. 82–94.
3. Designing Fire Protection for Steel Columns, Third Edition, American Iron and Steel Institute, Washington, DC, 1980.
4. "Standard Calculation Methods for Structural Fire Protection," ASCE/SEI/SFPE 29-99, American Society of Civil Engineers, Reston, VA, 1999.
5. International Building Code, International Code Council, Falls Church, VA, 2003.
6. NFPA 5000 – Building Construction and Safety Code, National Fire Protection Association, Quincy, MA, 2003.
7. Buchanan, A.H., Structural Design for Fire Safety, John Wiley & Sons, Chichester, 2001.
8. Milke, J.A., "Analytical Methods for Determining Fire Resistance of Steel Members," In: DiNenno P.J., ed., The SFPE Handbook of Fire Protection Engineering, Third Editon, National Fire Protection Association, Quincy, MA, 2002.
9. Jeanes, D.C., Technical Report 84-1, Society of Fire Protection Engineers, Boston, MA, 1984.